Heliyon 10 (2024) e31784

Contents lists available at ScienceDirect

Heliyon

journal homepage: www.cell.com/heliyon

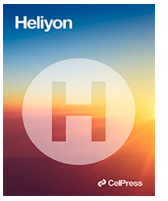

Research article

Purple sweet potato anthocyanins normalize the blood glucose concentration and restore the gut microbiota in mice with type 2 diabetes mellitus

Wei Mi [1], Zhiyong Hu [1], Shuying Zhao, Wei Wang, Wu Lian, Peng Lu, Tala Shi [*]

School of Public Health, Binzhou Medical University, Yantai, China

ARTICLE INFO

Keywords:
Purple sweet potato anthocyanins
Blood glucose concentration
Gut microbiota
Type 2 diabetes mellitus

ABSTRACT

Background: This study investigated the effects of purple sweet potato anthocyanins (PSPA) in a type 2 diabetes mellitus (T2DM) mouse model.

Methods: Sixty-five male mice were randomly divided into one control group and four experimental groups, which were fed with a high-fat diet and intraperitoneally injected with streptozotocin (STZ) to induce T2DM. The model mice were treated with 0 (M), 227.5 (LP), 455 (MP), or 910 (HP) mg/kg PSPA for ten days. ELISA, 16S rRNA sequencing, and hematoxylin and eosin staining were used to assess blood biochemical parameters, gut microbial composition, and liver tissue structure, respectively.

Results: The FBG concentration was significantly decreased in the LP (6.32 ± 1.05 mmol/L), MP (6.32 ± 1.05 mmol/L), and HP (5.65 ± 0.83 mmol/L) groups; the glycosylated hemoglobin levels were significantly decreased in the HP group (14.43 ± 7.12 pg/mL) compared with that in the M group (8.08 ± 1.04 mmol/L; 27.20 ± 7.72 pg/mL; $P < 0.05$). The PSPA treated groups also increased blood glutathione levels compared with M. PSPA significantly affected gut microbial diversity. The Firmicutes/Bacteroidetes ratio decreased by 38.9 %, 49.2 %, and 15.9 % in the LP, MP, and HP groups compared with that in the M group (0.62). The PSPAs treated groups showed an increased relative abundance of *Lachnospiraceae_Clostridium*, *Butyricimonas*, and *Akkermansia* and decreased abundance of nine bacterial genera, including *Staphylococcus*.

Conclusion: PSPA reduced blood glucose levels, increased serum antioxidant enzymes, and optimized the diversity and structure of the gut microbiota in mice with T2DM.

1. Introduction

The prevalence of diabetes mellitus (DM) is increasing and has become a prominent public health problem worldwide. According to the International Diabetes Federation, there will be approximately 537 million patients with DM worldwide in 2021 [1]. Approximately 850 billion dollars in global medical care will be spent on treating and healthcare patients with DM, imposing a significant burden on society and the health system. Approximately 12 % of adults in China have DM, with type 2 diabetes mellitus (T2DM) accounting for up to 95 % of cases [2]. T2DM is caused by a complex combination of external factors, such as an imbalanced dietary

* Corresponding author.
E-mail address: shitala@bzmc.edu.cn (T. Shi).
[1] These authors contributed equally to this work.

https://doi.org/10.1016/j.heliyon.2024.e31784
Received 10 March 2024; Received in revised form 8 May 2024; Accepted 22 May 2024
Available online 23 May 2024

structure, obesity, and a sedentary lifestyle [3]. The prevention and treatment of T2DM mainly involve comprehensive treatment, including diet, exercise, drugs, blood glucose monitoring, and DM education. Early dietary intervention has become the primary method for reducing T2DM morbidity.

Purple sweet potato anthocyanins (PSPA) are natural flavonoids and contain many varieties of anthocyanins. At present, Zhu et al. [4], used LC-PDA-APCI-MS to identify the anthocyanin structures of 10 Chinese purple sweet potatoes, they have cyanidin or paeoniflorin 3-sophoroside 5-glucoside, and its acylated derivatives being the main anthocyanins. The high acylated anthocyanin content provides color and greater stability and is directly absorbed into the bloodstream [5,6]. Previous studies have suggested that PSPA shows a plethora of biological activities, including antioxidant [7], anti-inflammatory [8] anticancer [9], and cardiovascular protective functions [10]. Many of these health benefits are attributed to the potent antioxidant activity of anthocyanins, which can protect DNA, proteins, and lipids from damage and activate specific detoxification enzymes, such as glutathione reductase, glutathione peroxidase, and glutathione S-transferase, to reduce oxidative stress [11]. This may be related to hydrogen atom and single-electron transfer, followed by proton transfer [12].

However, recent evidence suggests that the gut microbiota plays a key role in increasing the bioavailability of PSPA. Most anthocyanins reach the colon, interact with gut microbes, and are metabolized or de-glycosylated to monosaccharides and di-glycosides or decompose into glycosidic ligands [13]. Dysbiosis of the gut microbiota is associated with the development and progression of T2DM [14] and could lead to elevated levels of inflammation, increased insulin resistance, intestinal permeability, and altered mucosal immune responses [15]. Previous research has revealed that, compared with healthy subjects, patients with T2DM have obvious gut microbial dysbiosis, with the Firmicutes/Bacteroidetes ratio and harmful bacteria levels, including *Escherichia coli* increased, but decreasing levels of probiotic species, such as *Lactobacillus*, *Bifidobacterium*, and *Akkermansia* genera [16]. Therefore, regulation of the composition of the microbial community may be one of the primary mechanisms by which PSPA reduces blood glucose levels and prevents T2DM.

In this study, we investigated the biochemical indices and gut microbiota to determine whether PSPA exerts an anti-diabetic effect and protects against the adverse effects of diabetes. Commonly analyzed parameters, including serum blood glucose concentration, inflammatory factors, and gut microbial diversity, were analyzed by Enzyme-linked Immunosorbent Assay (ELISA) and 16SrRNA gene sequencing, and their relationships were assessed using Spearman's correlation analysis. These results provide evidence for the effects of PSPA on the pathogenesis of T2DM.

2. Materials and methods

2.1. Preparation of anthocyanins from purple sweet potato

Anthocyanins were prepared using a method described by Ref. [17]. Selected purple sweet potatoes (001; purchased from Shandong Yi Mu Sweet Potato Agricultural Science and Technology Co., Ltd., Shandong, China) were washed and cut into strips, dried in an oven for 12 h at 50 °C, crushed, passed through 100 mesh, and stored at 4 °C in the dark. PSPA extraction was performed using 0.1 % HCl-ethanol as the solvent (material-liquid ratio of 1:20, m/v) with the addition of 54 U/mL cellulase. After ultrasonic washes at 100 W and 51 °C for 30 min, the samples were centrifuged at 2500×*g* for 15 min. The resulting supernatant was removed and concentrated by rotary evaporation (55 °C, 150×*g*). The crude anthocyanin extract was purified using AB-8 microwell resin, washed, eluted with ethanol, and freeze-dried to obtain pure PSPA.

The anthocyanin monomers were determined from PSPAs using a Thermo Q Extractive high-performance liquid chromatography-mass spectrometry (QE LC-MS) system. The HPLC mobile phase consists of methanol containing acetonitrile (A) and 0.1 % formic acid aqueous solution (B), The detection wavelengths were set at 520 nm, and the column temperature is 25 °C. Mass spectrometry analysis conditions were set as follows: run time 10 min, full MS resolution with 70,000; AGC target 3e6, maximum IT 100 ms, scan range 100–2000 *m/z*, dd-ms/dd-SIM resolution with 17500; AGC target 1e5, maximum IT 50 ms, isolation window 4.0 *m/z*, collision energy of 20/30/40 in NCE mode. Finally, the MS/MS (*m/z*) fragmentations retention time and mass-to-charge ratio (*m/z*) indexes were compared with previously reported literature data [18,19].

2.2. Animal experiments

Sixty-five specific-pathogen-free male Kunming mice at eight weeks of age, with an average weight of 18∼20 g, were purchased from Jinan Pengyue (Shandong, China; Permit No: SYXK[Lu]-2019–0003), all experiments protocols complied with the care and use of laboratory animals in scientific investigations, and handling of animals were approved by the Ethics of Animal Use in Research Committee of Binzhou Medical Univesity (2022-361). The mice were adaptively fed under a conventional 12 h light/12 h dark cycle at 24 ± 1 °C and 40 %–60 % relative humidity. They were provided food and water *ad libitum*. After one week of acclimatization, the mice were randomly divided into five groups: control (C), model (M), low- (LP, 227.5 mg/kg), medium- (MP, 455 mg/kg), and high-dose (HP, 910 mg/kg) PSPA (13 mice in each group), the dosages of PSPA were referred to Ref. [20]. Group C was fed a maintained diet, the M, LP, MP, and HP groups were fed a high-fat diet (HFD), the energy supply ratio of protein, fat, and carbohydrate are 20.6 %, 12 %, 67.4 %, and 19.07 %, 60.34 %, 20.59 %, respectively. The fed was purchased from Beijing Keao Cooperation Feed Co., Ltd. (Beijing, China), and the components of maintain fed and high fat fed are listed (Supplementary Table 1). After four consecutive weeks, all mice were starved for 12 h, and group C received a citrate buffer; the M, LP, MP, and HP groups were intraperitoneally injected with 30 mg/kg streptozotocin (STZ; Sigma, St Louis, MO, USA) dissolved in 0.1 mol/L citrate buffer (pH 4.4), for three consecutive days. On the fourth day, fasting blood glucose (FBG) concentrations were determined, in each group, in 6∼7 mice FBG concentrations were higher

than 11.1 mmol/L, which confirmed as a T2DM model. Successfully modeled mice (6–7 mice/group) were intragastrically administered different doses of PSPA for ten days, and blood, liver tissue, and fecal samples were collected for further analysis.

2.3. Measurement of body weight, water intake, and food consumption

All experimental mice's water intake, food consumption, and body weight were recorded before and after the PSPA intervention. Water and food consumption were calculated using the formula: (total intake weight per cage)/(mice per cage).

2.4. Measurement of serum biochemical indices

FBG concentrations were recorded three days after STZ administration. On the final day of PSPA administration, blood samples were collected from the tail veins of the mice, and FBG concentrations were measured using a glucometer (Yuwell, Jiangsu, China). At the end of the experimental period, blood samples were collected by stripping the eyeball, and serum samples were collected after centrifugation at 1500×*g* for 15 min at 4 °C. The glycated hemoglobin (GHb), glutathione peroxidase (GSH-PX), tumor necrosis factor-α (TNF-α), lipopolysaccharide (LPS), and interleukin-6 (IL-6) concentrations were then tested using ELISA kits (Shanghai Jianglai Biological Technology Co., Ltd.), strictly following the manufacturer's instructions.

2.5. Liver histological analysis

Fresh liver tissues were fixed in 4 % paraformaldehyde, dehydrated in a gradient ethanol series, cleared in xylene, and embedded in paraffin. The tissue blocks were then cut into 5 μm sections, stained with hematoxylin and eosin (HE), and visualized by optical microscopy (Eclipse E100; Nikon, Tokyo, Japan). Then semi-quantitative analysis was followed by Image Pro Plus 6.0 software (Media Cybernetics, USA).

2.6. Gut microbiota analysis

Feces samples were collected in a sterile tube under aseptic conditions by cutting the colon and stored at −80 °C. Fecal whole-genome DNA was extracted, and the DNA purity was determined using 1 % agarose gel electrophoresis. DNA samples were diluted to 1 ng/μL, and the V3+V4 region was amplified by polymerase chain reaction (PCR). The PCR products were detected by 2 % agarose gel electrophoresis and purified using a Gel Recovery Kit (Qiagen, Hilden, Germany). Finally, a sequencing library was constructed using a TruSeq DNA PCR-Free Sample Preparation Kit (Illumina, San Diego, CA, USA). After quantification using a Qubit instrument (Invitrogen, Carlsbad, CA, USA), the library was sequenced on a NovaSeq 6000 instrument using a PE250 kit (Illumina). Bacterial richness and diversity were evaluated using Chao1 and Faith's polydiversity indices, and differences in microbiota communities between groups were analyzed using the unweighted pair–group method with arithmetic means (UPGMA) and partial least squares discriminant analysis (PLS-DA). Linear discriminant analysis (LDA) was performed to identify the key bacterial taxa that differed between groups (log10 > 2.0).

2.7. In vitro cultivation condition

We performed *in vitro* cultivation and PSPA intervention for the *Staphylococcus aureus* ATCC6538 strain (obtained from the Microbiology Research Center of the Chinese Academy of Sciences) to further verify the animal experimental results. Luria-Bertani Broth (LB Broth, Qingdao Haibo Biotechnology Co., Ltd) with 0, 30, or 90 μg/mL of PSPA was used as the culture broth. The pre-cultivated *Staphylococcus aureus* ATCC6538 in phosphate buffer saline (PBS) was added to 5 ml LB broth as optical density 600 nm (OD 600 nm) is 0.3, then incubated at 37 °C for 48 h, under semi-anaerobic conditions. The OD 600 nm was measured every 12 h, the measured data at 0 h, 0 μg/ml were normalized to Zero, and then the level of strain OD 600 nm at different times and broth conditions.

2.8. Statistical analysis

Biochemical data ($n = 6$) were analyzed using SPSS software (version 24.0; IBM, Armonk, NY, USA), and the data are represented as the mean ± standard deviation (SD). Differences between groups were computed using the Kruskal-Wallis rank-sum test or the R language Dunn's test. Spearman's correlation analysis used the R package (v4.0.0) to evaluate the relationships between bacterial genera and physiological parameters. Statistical significance was set at $P < 0.05$.

3. Results

3.1. PSPA content and composition

The semi-purified anthocyanins in experimental purple potatoes is 120 mg/100 g. LC-MS results compared with previous published fragments information, we get 10 different types of anthocyanins, which include Cyanin-3-(6-caffeic acid 6-ferulic acid sophoroside)-5-glucoside, peonidin, cyanin 3-caffeoyl sophoroside 5-glucoside, chlorogenic acid, cyanin 3-caffeoyl, dicaffeioyl quinic acid, paeoniflorin-3-glucoside, anthocyanin 3-Hogwash flavor glycoside-5-glucoside, paeoniflorin 3-p-hydroxybenzoyl sophoroside 5-

glucoside, cyanin 3-p hydroxy benzoyl sophoroside 5-glucoside, but the amount of each anthocyanin monomers were not detected in present study (Supplementary Table 3).

3.2. Effects of PSPA on body weight, food intake, and water intake

As shown in Fig. 1, the experimental protocol was divided into two stages. Before the PSPA intervention, the high-fat diet increased feed intake and did not affect water intake or body weight. After PSPA treatment, the average water and feed intake per cage decreased with increasing PSPA doses. The body weights of group C and the four other groups were significantly different ($P < 0.05$), but there was no significant difference between the M and the LP, MP, or HP groups. However, after PSPA intervention, compared with that in the M group, the PSPA treated groups showed significantly decreased polydipsia, polyphagia, and more controlled body weights (Fig. 2A, B, and 2C). These results indicate that the T2DM mouse model was successfully established and that PSPA intervention alleviated the common symptoms of T2DM.

3.3. Effect of PSPA on blood biochemical indices

FBG and GHb concentrations in the blood are significant indicators of T2DM. Compared with that in the M group (8.08 ± 1.04 mmol/L), the LP, MP, and HP groups had significantly reduced FBG concentrations ($P < 0.05$). The MP group had the lowest FBG concentration (5.72 ± 0.70 mmol/L). The GHb concentration reflects recent blood glucose concentrations. The GHb concentration was significantly higher in the M group (27.20 ± 7.72 pg/mL) than in the C group (12.77 ± 6.18 pg/mL; $P < 0.05$); however, compared with that in the M group, the LP, MP, and HP groups had decreased GHb concentrations. The HP group showed the lowest GHb concentration (14.43 ± 7.12 pg/mL; $P < 0.05$) (Table 1).

The inflammatory factors LPS, TNF-α, and IL-6 are associated with T2DM. In this study, the levels of inflammatory factors were higher in the M group than in the C group, and PSPA intervention reduced the levels of inflammatory factors; but, this difference was not statistically significant. In addition, the GSH-PX concentration was significantly higher in group C (56.02 ± 0.49 pg/mL) than in the M group (34.54 ± 1.29 pg/mL; $P < 0.05$), indicating that T2DM reduced serum GSH-PX concentrations and indirectly damaged the structure and function of the cell membrane. However, compared with that in the M group, the LP, MP, and HP groups showed a significant dose-dependent increase in GSH-PX concentration ($P < 0.05$), and the HP group showed the highest serum GSH-PX concentration (50.46 ± 1.03 pg/mL). These results indicated that a high dose of PSPA had a better modulatory effect on the oxidation status of T2DM mice (Table 1).

3.4. Effect of PSPA on liver tissue

The liver histological structure in group C exhibited normal hepatic architecture with normal hepatocyte morphology and an orderly arrangement of hepatic cell cords. However, the M group had multiple focal liver cell necrosis, nuclear dissolution, and replacement by proliferative connective tissue, accompanied by lymphocyte infiltration; Mild liver cell steatosis, and small circular vacuoles visible in the cytoplasm. The PSPA intervention had a positive effect on these pathological changes, the hepatocytes showed a few lipid vacuoles and a small amount of lymphocyte infiltration or not. Furthermore, Semi-quantitative analysis was conducted for hepatocellular lipid droplets, inflammatory foci, and fat degeneration, the liver pathological scores were shown by the sum of the above scores. Compared with group C, the pathological score of M group mice was significantly increased, but compared with the M group, the pathological scores of the MP, and HP significantly decreased ($P < 0.05$). (Fig. 3).

3.5. Effect of PSPA on gut microbial diversity

After quality filtration of the 16S rRNA sequencing data, we obtained 2,076,249 clean reads from the 30 samples, and an average of $69,208 \pm 5953$ reads were generated per sample. Valid sequences were clustered as operational taxonomic units (OTUs). The average annotated OTU number in the five groups was 505×105, and the top 50 assigned OTUs are shown in the phylogenetic tree (Fig. 4A).

In α diversity analysis, the rarefaction curve for each group showed a gentle slope, and coverage surpassed 99.6 %, indicating that the sequencing data were reliable (Fig. 4B). The gut microbial community richness and diversity of the groups were measured using Chao1, Shannon, Simpson, and Faith poly diversity indices. The Chao1, Shannon, and Simpson microbial richness results showed no

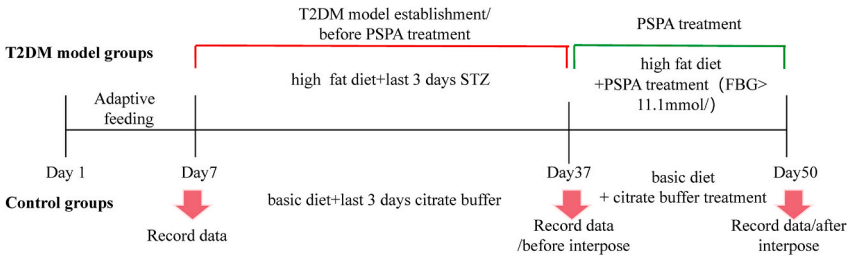

Fig. 1. Chart of experimental protocol.

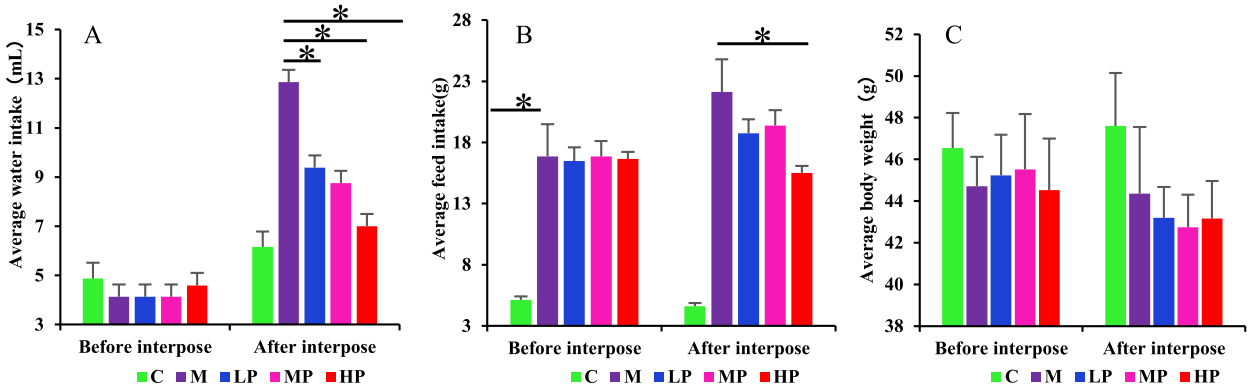

Fig. 2. PSPA effect on typical clinical symptoms. (a) Changes in water intake. (b) changes in feed intake. (c) body weight changes during different experimental periods. X-axis experimental periods, Y-axis, average water intake, feed intake, and body weight for each group. *, indicate significant differences between groups ($P < 0.05$). C: control group; M: model group; LP: low dose PSPA intervention group; MP: medium dose PSPA intervention group; HP: high dose PSPA intervention group.

Table 1
Changes in serum biochemical indexes.

Groups	FBG (mmol/L)	GHb (pg/mL)	LPS (pg/mL)	TNF-α (pg/mL)	IL-6 (pg/mL)	GSH-PX (pg/mL)
C	8.61 ± 0.35	13.07 ± 5.57	16.27 ± 0.50	11.58 ± 0.64	1.65 ± 0.17	56.02 ± 0.49#
M	8.08 ± 0.95	29.20 ± 4.82*	16.57 ± 0.86	12.50 ± 0.93	1.68 ± 0.15	34.54 ± 1.29*
LP	6.09 ± 0.85*	23.34 ± 13.47*	16.49 ± 0.48	12.14 ± 0.40	1.61 ± 0.06	45.46 ± 1.48*#
MP	6.74 ± 1.28*#	18.01 ± 6.76	16.36 ± 0.66	12.15 ± 1.06	1.59 ± 0.07	46.83 ± 1.42*#
HP	5.97 ± 1.05*#	14.43 ± 7.12#	16.14 ± 0.17	12.00 ± 0.31	1.61 ± 0.62	50.46 ± 1.03*#
F	89.855	3.515	0.443	1.254	0.420	217.803
df	247	29	24	29	29	24
P	0.000	0.021	0.776	0.314	0.793	0.000

*$P < 0.05$, compared with C group; #$P < 0.05$, compared with M group; FBG: Fasting Blood Glucose, LPS: Lipopolysaccharide, TNF- α: Tumor Necrosis Factor- α, GHb: glycated Haemoglobin, GSH-PX: Glutathione Peroxidase, IL-6: Interleukin-6 (N = 6). C: control group; M: model group; LP: low dose PSPA intervention group; MP: medium dose PSPA intervention group; HP: high dose PSPA intervention group.

statistical differences among the groups (Fig. 4C); however, Faith's poly diversity analysis showed significant differences among the M, LP, MP, and HP groups ($P < 0.05$). These results indicate that PSPA intervention did not affect microbial richness or alter gut microbial diversity in T2DM mice (Fig. 4D).

PLS-DA was used to analyze *β*-diversity, and according to the PLS-DA coordinate graph and the area under the curve, there were significant differences in the gut microbial structure among the five experimental groups (Fig. 4E and F). Group C clustered separately from group M, and the LP, MP, and HP groups showed evident separation in microbial community structure. These results suggest that PSPA treatment reshaped the gut microbial structure of T2DM mice.

3.6. Effect of PSPA on the taxonomic composition of the gut microbiota

Twenty-two phyla were annotated from the sequencing data, and the Kruskal-Wallis test results showed that the relative abundances of Bacteroidetes, Firmicutes, Actinobacteria, and Cyanobacteria were significantly different between the groups. Compared with that in group C, the relative abundances of Actinobacteria and Firmicutes decreased by 87.5 % and 38.5 %, respectively, and the abundances of Bacteroidetes and Cyanobacteria increased by 95.5 % and 41.8 %, respectively, in the M group. However, compared with that in the M group, the LP, MP, and HP groups showed 38.9 %, 49.2 %, and 15.9 % reductions in the Firmicutes/Bacteroidetes ratios (Fig. 5A and B).

Two hundred and eighteen genera were annotated, and the Kruskal-Wallis rank-sum test showed that 23 genera were significantly different between the groups. Compared to that in the M group, the LP group showed increased abundances of *Lachnospiraceae_Clostridium*, *Aerococcus*, *Lactococcus*, *Coprobacillus*, *Butyricimonas*, *Jeotgalicoccus*, *Arthrobacter*, *Prevotella*, and *Bacteroides*, with values of 99.0 %, 89.2 %, 83.3 %, 68.3 %, 54.7 %, 42.6 %, 2.2.2 %, 12.8 %, and 4.3 %, respectively. In the MP group, *Lachnospiraceae_Clostridium*, *Butyricimonas*, *Prevotella*, *Coprobacillus*, and *Desulfovibrio* accounted for 63.6 %, 54.8 %, 31.7 %, 23.2 %, and 3.7 % of the bacteria, respectively. In the HP group, the abundances of *Lachnospiraceae_Clostridium*, *Butyricimonas*, and *Desulfovibrio* were 98.6 %, 66.8 %, and 55.1 %, respectively. The LP, MP, and HP groups showed reduced abundances of *Staphylococcus*, *Enterococcus*, *Corynebacterium*, *Streptococcus*, *Prevotellaceae_Prevotella*, *Lactobacillus*, *Psychrobacter*, *Acinetobacter*, and *Flexispira* (Fig. 5C). In addition, multiple comparisons between the two groups using the DESeq2 method revealed that the LP, MP, and HP groups had significantly increased *Akkermansia* abundance ($P < 0.05$) and reduced *Staphylococcus*, *Pseudomonas*, *Holdemania*, and *Serratia* abundances (Fig. 5D,

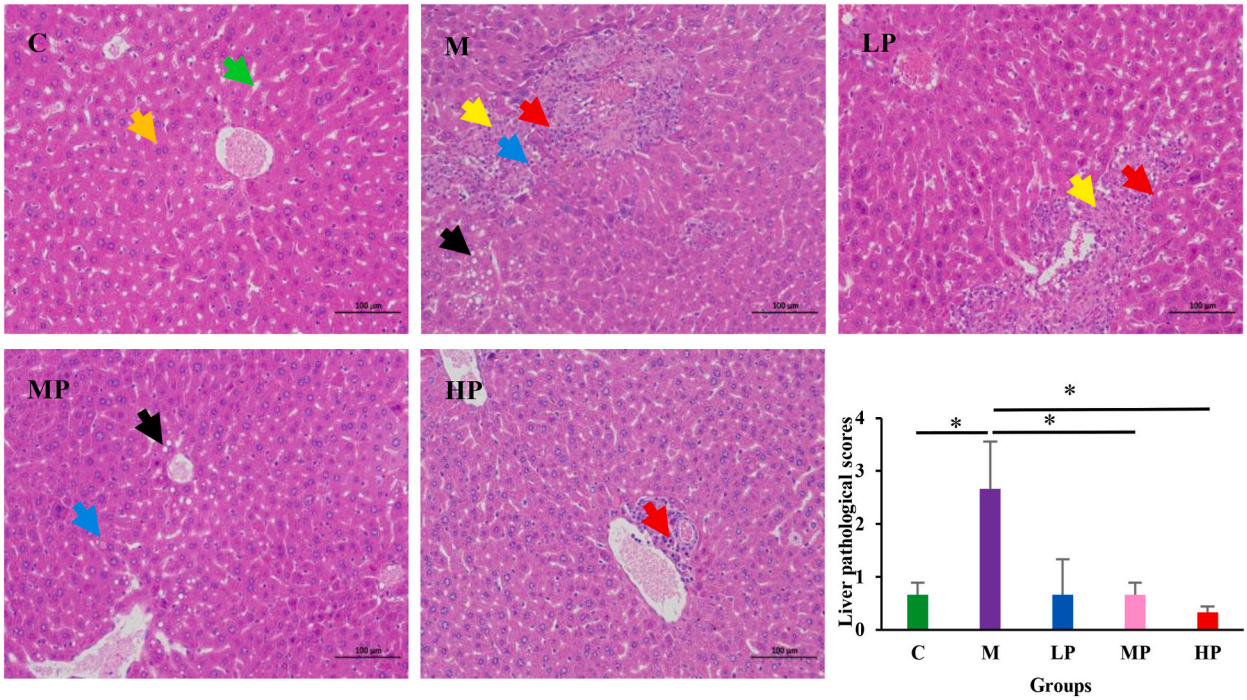

Fig. 3. Effects of PSPA treatment on liver histopathologic alterations examined by H&E staining (magnification: 200 ×). Orange arrow, normal hepatocytes; Green arrow, normal hepatic sinus; Yellow arrow, hepatocellular necrosis, and dissolution, replaced by proliferative connective tissue; Red arrow, Lymphocyte infiltration; Black arrow, hepatocellular steatosis; Blue arrow, hepatocellular necrosis. C: control group; M: model group; LP: low dose PSPA intervention group; MP: medium dose PSPA intervention group; HP: high dose PSPA intervention group. *P < 0.05. (For interpretation of the references to color in this figure legend, the reader is referred to the Web version of this article.)

E, and 5F).

In addition, linear discriminant effect size (LDA >2) analysis results showed that group C had ten characteristic genera, including *Staphylococcus*, *Lactobacillus*, and *Prevotella*; the M group had *Enterococcus* and *Proteus*; the LP group had *Akkermansia* and *Clostridium*; the MP group had *Prevotella*, *Cetobacterium*, and *Serratia*; and the HP group had *Desulfovibrio* as the dominant bacterial genera (Fig. 5G and H). The results of these different types of analyses indicated that different doses of PSPA increased the number of beneficial bacteria in the mouse intestine and reduced the relative abundance of pathogenic or opportunistic pathogens such as *Staphylococcus*.

To further verify the animal experimental results, we performed *in vitro* cultivation and PSPA intervention for *Staphylococcus aureus* (*Staphylococcus aureus* ATCC6538). LB broth with 0, 30, or 90 μg/mL of PSPA was used as the culture broth, and *Staphylococcus aureus* ATCC6538 was incubated under semi-anaerobic conditions at 37 °C for 48 h. The results indicated that PSPA inhibited the growth and reproduction of the *Staphylococcus aureus* strain ATCC6538. After 48 h of co-cultivation, the 30 μg/mL and 90 μg/mL inhibition rates were 30.1 % and 35.3 %, compared with 0 μg/mL. These results are consistent with those of the animal studies, indicating that PSPA intervention can ameliorate infectious diseases caused by *Staphylococcus* spp. and protect the digestive system (Fig. 5I).

3.7. Correlation of bacterial genus and biochemical indicators

Spearman's correlation analysis of significantly different bacterial genera and serum biochemical indices showed that FBG concentration was positively correlated with *Corynebacterium*, *Acinetobacter*, *Prevotellaceae_Prevotella*, *Flexispira*, *Leuconstoc*, and *Holdemania* abundance, which decreased after the PSPA intervention. The GHb concentration was negatively correlated with the abundance of *Roseburia*. The serum GSH-PX concentration was positively correlated with *Lachnospiraceae_ Clostridium*, *Aerococcus*, and *Jeotagallicoccus* abundance, which significantly increased after PSPA intervention; however, it was negatively correlated with *Bacteroides* abundance (r less than or greater than 0.6, $P < 0.01$). These results indicated that the increase in blood glucose concentration caused by T2DM may be related to the increased levels of six bacterial genera, including *Prevotellaceae* and *Prevotella*, and that the decrease in GSH-PX concentration induced by T2DM was related to the increased relative abundance of *Bacteroides* (Fig. 6A).

However, the results of the correlation network analysis of the top 30 bacterial genera showed that *Corynebacterium* abundance was positively correlated with a decrease in the abundance of bacterial genera after PSPA intervention, including *Streptococcus*, *Staphylococcus*, and *Flexispira*, and negatively correlated with *Prevotella*, *Akkermansia*, and *Butyricimonas*. *Lachnospiraceae_Clostridium* abundance was positively correlated with GSH-PX activity and negatively correlated with *Pseudomonas* abundance (Fig. 6B).

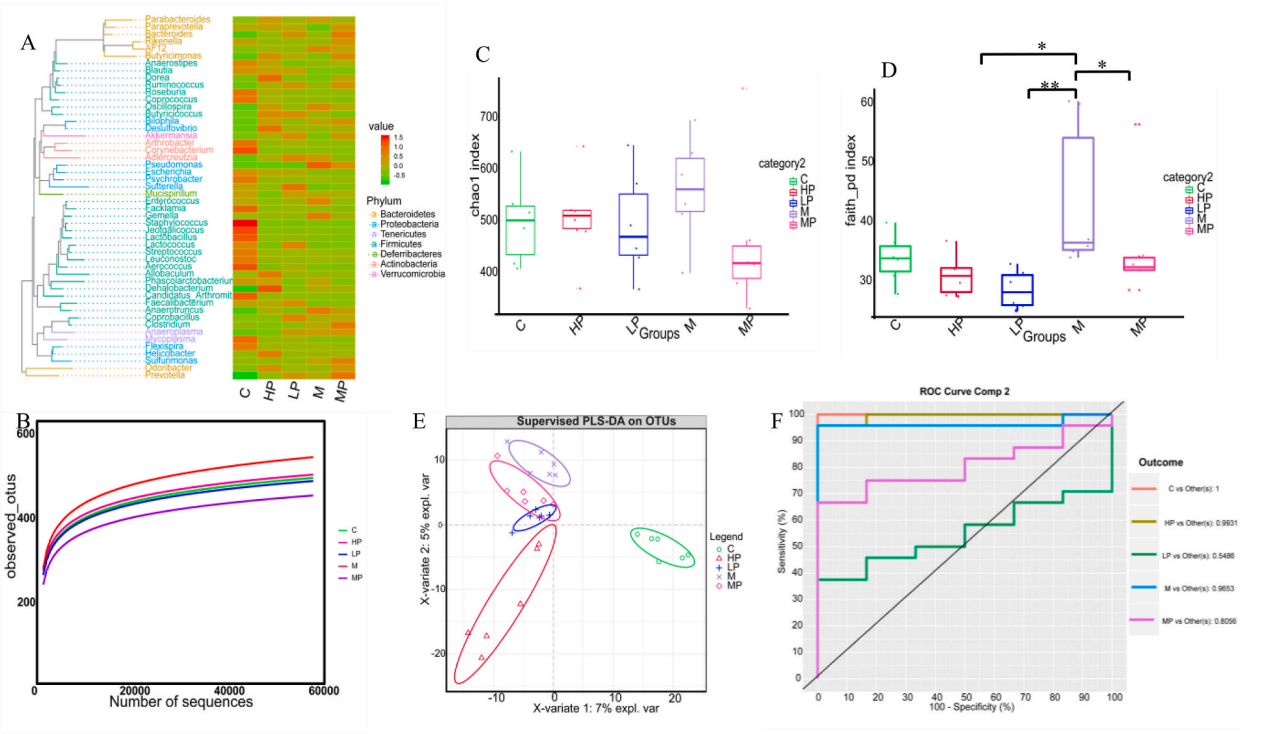

Fig. 4. PSPA effects on gut microbial diversity. (A) Top 50 OTU taxonomic phylogenetic tree analysis (n = 6 in each group). (B) Rarefaction analysis of samples from five groups. (C, D) Alpha diversity analysis, *P < 0.05, * *P < 0.01. (E, F) Beta diversity analysis. C: control group; M: model group; LP: low dose PSPA intervention group; MP: medium dose PSPA intervention group; HP: high dose PSPA intervention group.

3.8. Effect of the PSPA intervention on microbial function

Functional prediction analysis of the gut microbiota was performed with PICRUSt2, using data from the Metabolic Pathways From all Domains of Life (MetaCyc) and Kyoto Encyclopedia of Genes and Genomes (KEGG) databases. In the MetaCyc database, Dunn's test results show that compared with that in M Group, the LP, MP, and HP groups showed significantly reduced taxadiene biosynthesis (PWY-7392; 52.5 %, 57.4 %, 35.6 %); homolactic fermentation (ANAEROFRUCAT-PWY; 17.3 %, 30.0 %, 7.6 %); N-acetylglucosamine, N-acetylmannosamine, and N-acetylneuraminate degradation (GLCMANNANAUT-PWY; 36.0 %, 47.0 %, 20.7 %); and pyrimidine deoxyribonucleosides degradation (PWY0-1298; 21.8 %, 38.2 %, 11.5 %; $P < 0.05$) and increased methylerythritol phosphate pathway I and II, (NONMEVIPP-PWY, PWY-7560; 8.7 %, 9.3 %, 13.3 %), the super pathway of geranyl diphosphate biosynthesis II (PWY-5121; 8.1 %, 8.2 %, 12.3 %), UMP biosynthesis (PWY-5686, 7.9 %, 8.6 %, 12.3 %), chorismate biosynthesis from 3-dehydroquinate (PWY-6163; 6.6 %, 8.0 %, 12.2 %), and NAD biosynthesis I from aspartate (PYRIDNUCSYN-PWY; 15.8 %, 16.7 %, 16.7 %) (Fig. 7A and B). In the KEGG database, ANOVA analysis results showed that, compared with that in the M group, the intervention significantly reduced 13 types of pathways and increased 16 types. Further Duncan test analysis for the above 29 kinds of pathways analysis results show the LP, MP, and HP decreased the abundance of *Staphylococcus aureus* infection, phosphotransferase system, dioxin degradation, naphthalene degradation; however, increased PI3K-Akt signaling pathway, Th17 cell differentiation, Carotenoid biosynthesis, antigen processing presentation, estrogen signaling pathway, and novobiocin biosynthesis (Fig. 7C).

4. Discussion

Lower glucose tolerance, higher FBG concentrations, insulin resistance, polydipsia, increased food intake, and dyslipidemia are typical clinical symptoms and basic pathological characteristics of T2DM [21]. Effective control of blood glucose concentration is crucial for preventing diabetic complications and improving the quality of life for patients with T2DM [22]. Previous studies have shown that ob/ob mice treated with apple proanthocyanidin for eight weeks had significantly reduced blood glucose concentrations [23]. Cacao bean proanthocyanidins stimulate glycogen synthesis and glucose absorption [24]. In this study, PSPA intervention significantly decreased FBG and GHb concentrations without affecting body weight and reduced water intake compared to that in the M group. In consist to our study, the purple potato extracts of the Blue Congo variety also lowered blood glucose, improved glucose tolerance, and decreased the amount of GHb of STZ-induced diabetic rats [25]. Those results indicated that PSPA inhibits appetite, reduces polydipsia symptoms, and reduces blood glucose concentrations in mice with DM, which may be attributed to an improved balance between glucose absorption and utilization [26].

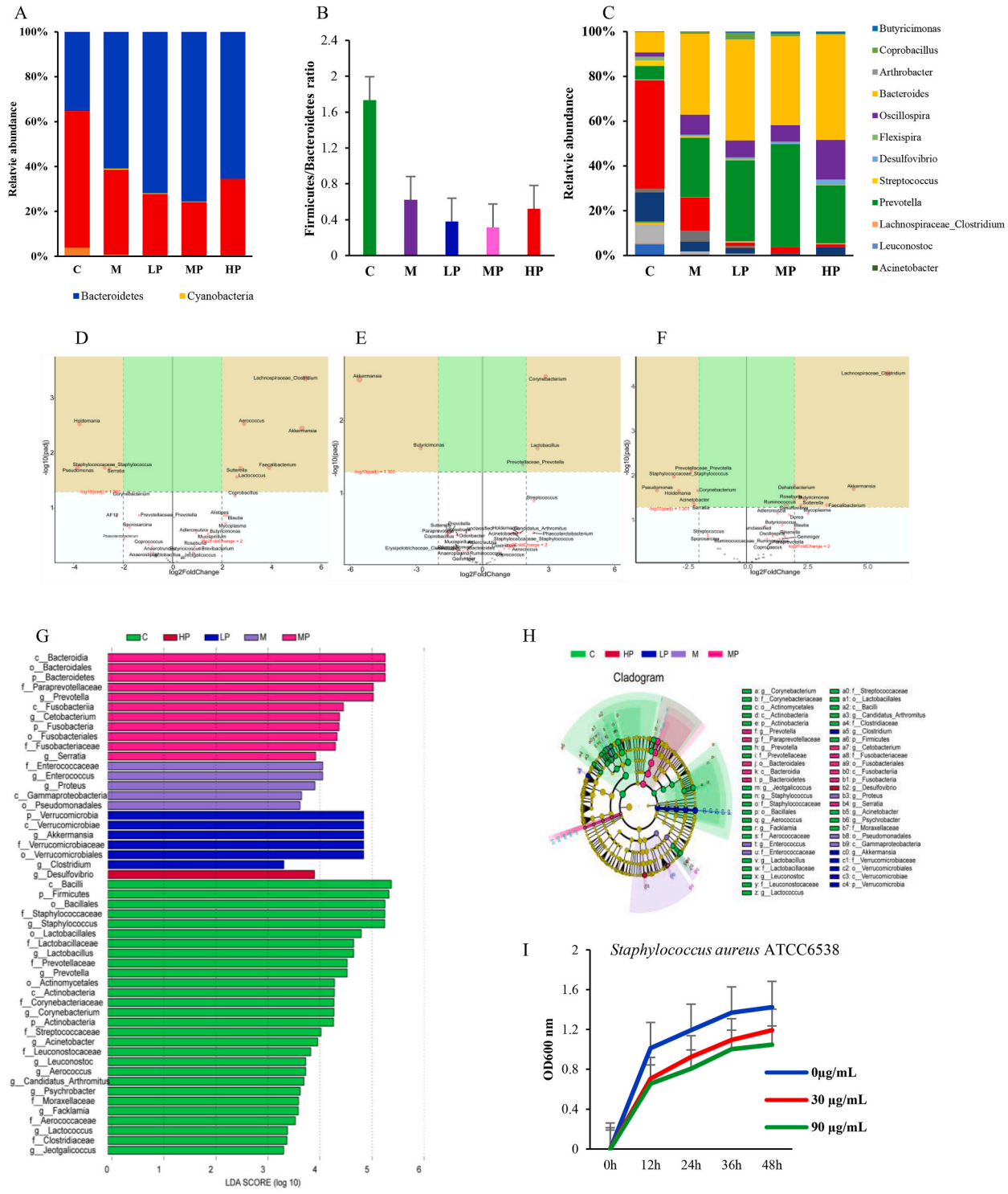

Fig. 5. Effects of PSPA on gut microbial composition. (A) Significantly different bacterial phylum between groups. (B) Firmicutes/Bacteroides ratio changes. (C) Significantly different bacterial genus between groups. (D, E, F) Multiple comparisons between the two groups using the DESeq2 method. (D) Comparison between LP and M. (E) Comparison between M and MP. (F) Comparison between HP and M. (G, H) Linear discriminant analysis effect size (LDA >2) analysis. (I) PSPA effect on *Staphylococcus aureus* ATCC6538 at *in vitro* cultivation conditions, *, indicates a significant difference compared with that in non-PSPA intervention groups ($P < 0.05$). C: control group; M: model group; LP: low dose PSPA intervention group; MP: medium dose PSPA intervention group; HP: high dose PSPA intervention group.

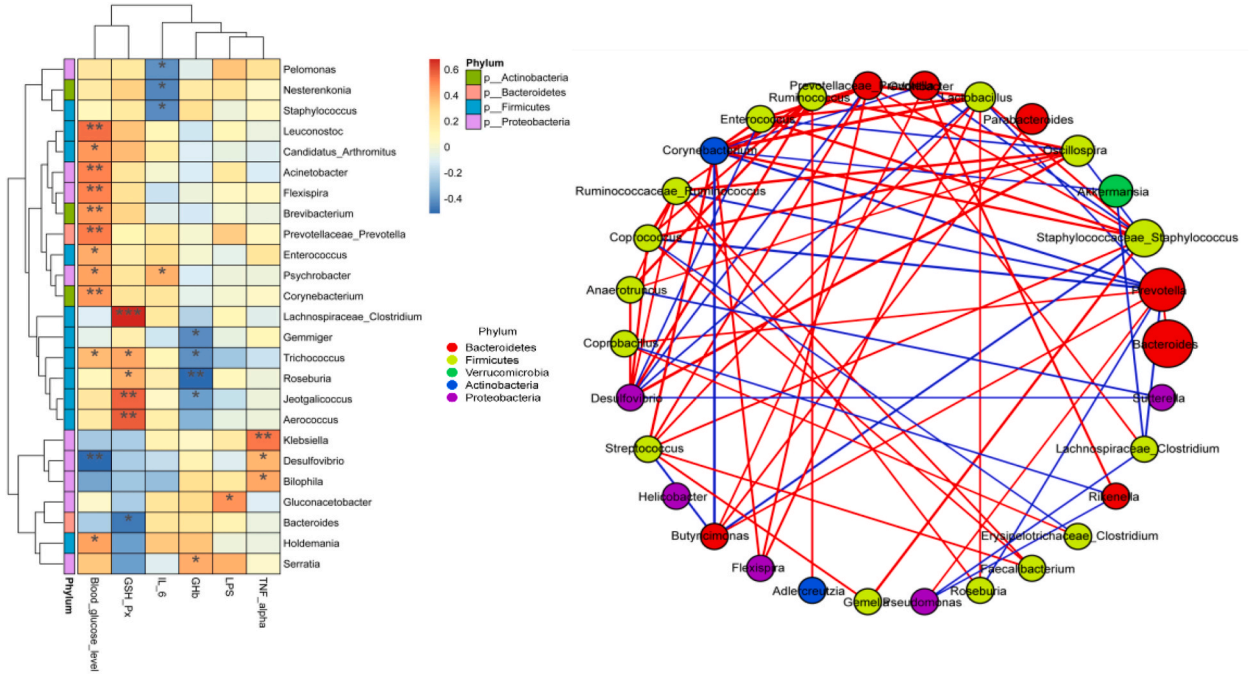

Fig. 6. (A) Heatmap of the correlation between significantly different gut microbial genera and biochemical indices. *P < 0.05, **P < 0.01, ***P < 0.001, FBG: fasting blood glucose; LPS: lipopolysaccharide; TNF-α: tumor necrosis factor-α; GHb: glycated hemoglobin; GSH-PX: glutathione peroxidase; IL-6: interleukin-6. (B) correlation between significantly different bacteria genera.

Diabetes is associated with excessive production of reactive oxygen species, leading to liver oxidative damage and defects in insulin action and secretion [27]. GSH-PX is the most critical endogenous substance in cells that can remove low-molecular-weight free radicals, hydrogen peroxide, and lipids [28]. Therefore, measuring GSH-PX activity can indirectly reflect the degree of damage to organ function in diabetic mice. In our study, after PSPA intervention, the GSH-PX concentration in mouse serum significantly increased, which helped maintain homeostasis in the physiological environment to a certain extent [20]. reported a similar effect, showing that a high dose of PSPA extract (917 mg/kg body weight) increased the antioxidant capacity (catalase, GSH-PX, and superoxide dismutase activities) and reduced malondialdehyde concentration in the serum and liver of obese mice. These results indicate that increasing antioxidant capacity reduces the effects of inflammatory factors resulting from a high-fat diet that causes obesity, or T2DM. The increase in GSH-PX concentration positively correlated with the abundance of five bacterial genera, which significantly increased in the PSPA-treated group. These results indicate that increasing the abundance of *Lachnospiraceae_Clostridium* can increase serum GSH-PX concentrations. That antioxidant enzyme may inhibit the generation of advanced glycation end products [29], reduce oxidative stress and the damage or inflammation caused by free radicals in pancreatic β cells [30], and prevent the onset of diabetes.

In addition, the gut microbiota is recognized as a key environmental factor contributing to the pathophysiology of T2DM [31,32]. Dysbiosis of the gut microbiota leads to disruption of the gut epithelium and microbial diversity, increasing the production of inflammatory factors associated with diabetes and insulin resistance [33]. A disrupted ratio of Firmicutes to Bacteroidetes leads to impaired glucose metabolism [34], human studies have revealed that patients with T2DM have increased Firmicutes and decreased Bacteroidetes levels, resulting in higher Firmicutes/Bacteroidetes ratios [35]. Decreasing the abundance of Firmicutes and increasing the proportion of Bacteroidetes reduces inflammation. In this study, we observed a decrease in the concentrations of inflammatory factors (LPS, TNF-α, IL-6) and the Firmicutes/Bacteroidetes ratio in the LP, MP, and HP groups compared with that in the M group. Moreover, Liu et al. [21] reported that PSPA extract decreased the Firmicutes/Bacteroidetes ratio, reduced serum LPS, TNF-α, and IL-6 concentrations, and normalized gut microbial diversity in a high-fat-diet-fed obese mouse. The above results indicate that PSPA or its microbial metabolites may protect the gut epithelium or the gut microbial structure and thus reduce inflammatory factor production. According to Spearman's correlation analysis, IL-6, LPS, and TNF-α concentrations were positively correlated with *Psychrobacter*, *Gluconacetobacter*, *Bilophila*, and *Klebsiella* abundance; however, the abundance of these bacterial genera decreased after the PSPA intervention. Similar results were also reported by Dong et al. [36], the PSPA extract has a protective effect from *Klebsiella pneumoniae* infection and dampened inflammatory responses. So decreasing the abundance of pathogenic or conditional pathogenic bacteria may be one of the pathways to control the production of inflammatory factors, and assist for probiotic growth. Animal studies have shown that T2DM is associated with a decreased abundance of *Bacteroides* and *Akkermansia muciniphila* [37,38]. In this study, significantly higher levels of probiotic species, including *Lachnospiraceae_Clostridium*, *Akkermansia,* and *Butyricimonas*, were observed in the LP, MP, and HP groups, and the genus *Akkermansia*, *Faecalibacterium*, *Bacteroides*, *Roseburia,* and *Bifidobacterium* were negatively correlated with T2DM. The Lachnospiraceae family (Firmicutes phylum) can produce acetate, butyrate, and antibiotics and convert primary bile acids to secondary bile acids against drug-resistant pathogens [39,40]. Previous studies from animals and humans point to the

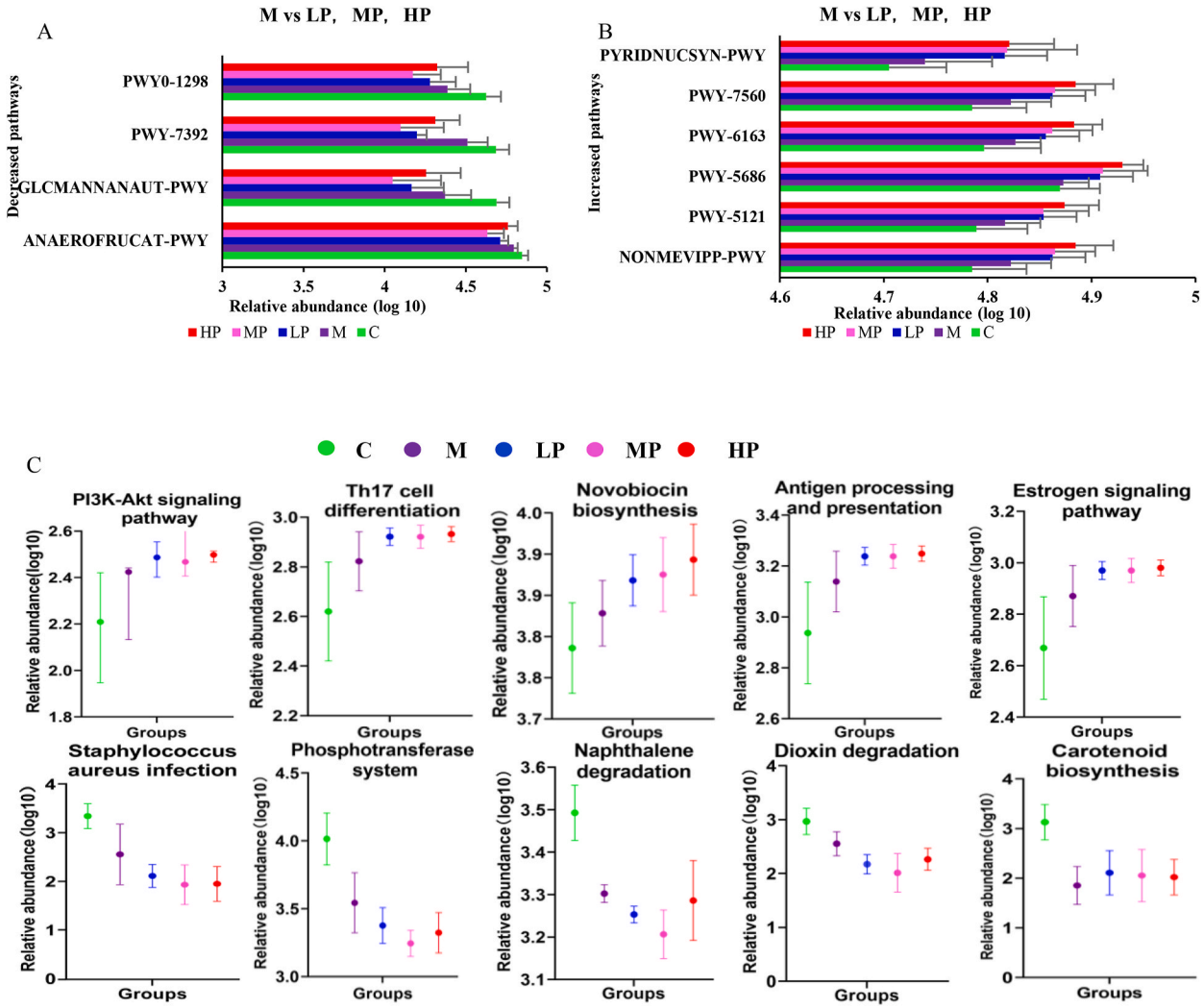

Fig. 7. Gut microbial functional prediction by PICRUSt2 using data from the MetaCyc and KEGG databases. (A, B) Significantly different pathways and enzymes between groups according to the MetaCyc database. (C) Significantly different pathways between groups according to the KEGG database. C: control group; M: model group; LP: low dose PSPA intervention group; MP: medium dose PSPA intervention group; HP: high dose PSPA intervention group.

reduction of butyrate-producing bacteria, such as *Faecalibacterium* and *Roseburia*, as one of the most important features responsible for the onset and development of T2DM [41]. *Bacteroides* preserve intestinal wall integrity by upregulating tight junctions' expression and reducing LPS production. *Akkermansia* has been proposed as an anti-diabetic strategy given its ability to decrease lipid accumulation, reduce serum LPS concentrations, and enhance gut barrier function, insulin secretion, and glucose tolerance [42–44]. Plovier et al. [45], demonstrated the application of *Akkermansia muciniphila* specific membrane proteins in obese mice with diabetes significantly reduces the fat content and improves insulin resistance and dyslipidemia, but reduces liver damage and inflammation-related plasma markers. *Butyricimonas* (Bacteroidetes phylum) can convert glucose to isobutyrate and n-butyrate, which may be a metabolic pathway, and PSPA decreases host blood glucose [46,47]. In addition, Sun et al. [48] reported that peonidin-based anthocyanins extracted from purple sweet potatoes inhibit the growth of *S. aureus* and *Salmonella typhimurium*. In the DSS-induced colitis mice model, PSPA extract significantly decreased *Escherichia/Shigella*, *Helicobacter*, and *Staphylococcus* [49]. Dwarf blueberry anthocyanins have excellent inhibitory effects on the growth of *E. coli* O157:H7, *S. aureus*, and *Listeria monocytogenes* [50]. In consistent with previous studies, our work also indicates the PSPA specific effect on the growth of pathogenic or opportunistic pathogenic bacteria, could inhibit the colonization of *Staphylococcus*, *Streptococcus* and seven other bacteria genera. The mechanisms by which anthocyanins inhibit the growth of harmful bacteria are attributed to the inhibition of enzyme synthesis, causing the bacteria to die eventually, or through interference with energy synthesis by harmful bacteria [51].

The anthocyanin action mechanisms in diabetes are related to certain enzymes (α-amylase and glucosidase), membrane receptors (FFAR1, GLP-1R), and genes involved in insulin-glucose signaling pathways, glucose transporter type 4 (GLUT4), peroxisome

proliferator-activated receptor (PPAR) genes [30]. In the KEGG functional prediction analysis, we observed a decreased *Staphylococcus aureus* infection pathway, which is consistent with decreased bacteria *Staphylococcus* genus, decreasing the pathogenic or opportunistic pathogenic bacteria-related pathway and gene expression may be one of the mechanisms of PSPA affecting T2DM. Interestingly compared with the M group, LP, MP, and HP groups had enrichment of the PI3K-Akt signaling pathway, which plays an important role in the metabolic effect of insulin, mediating glucose uptake, and lipid metabolism [50]. Insulin binds to the insulin receptor and is combined with PI3K to activate protein AKT and participates in the metabolic pathways of glucose transport and glycogen synthesis [52]. The imbalance of short-chain fatty acid (SCFA) in the gut plays a role in the development of diabetes mellitus, acts as a ligand and binds the cell surface membrane to induce intracellular signaling activity. Xia et al. [53] conducted molecular docking studies of SCFA and IGF1, PI3K, and AKT proteins, and found that SCFA is capable of binding with IGF1, PI3K, and AKT, and activating the PI3K/AKT signaling pathway, to reach the blood glucose lowing effects and insulin signal transduction. The present study missed the SCFA data of the samples, but the microbial community changes show a higher abundance in SCFA-producing bacteria genera after PSPA intervention, so it may be another way PSPA controls blood glucose levels. Studies found the mechanisms of SCFA in diabetes are via secretion of several gut hormones, G-protein coupled receptors (GPR) activation, and signal transduction [54,55]. Humans and rodents [56,57] studies reported that acetate, propionate, and butyrate increased glucagon-like peptide-1 (GLP-1) hormone, which binds to GLP-1 receptor to stimulate insulin secretion, but the anorectic hormone peptide YY was response to propionate, then regulate energy homeostasis and glucose metabolism. however, the activation of GPR40 (FFAR1) and glucokinase (GK) by anthocyanins could promote insulin secretion and hepatic glucose uptake in pancreatic cells and hepatocytes [58]. Results suggested that the PSPA intervention may change the gut microbial metabolites, like SCFA, branched-chain amino acid, and bile acid, which have positive effects on gut and liver tissue, decrease the inflammations, and protect from T2DM [59].

5. Conclusions

PSPA normalized blood glucose levels and reduced glycated hemoglobin and F/B ratio, but improved gut beneficial bacteria genera, while harmful bacteria genera were reduced. The increased beneficial genus abundance was positively correlated with blood GSH-PX but negatively correlated with GHb. In addition, functional prediction analysis showed decreased abundance in the *Staphylococcus aureus* infection pathway which may explain the reduction of Staphylococcus genus degradation. However, the present study defects the oral glucose tolerance test and insulin tolerance test, and further mRNA level determination of PI3K/AKT and gene expression analysis. The pathogenesis of T2DM is complex, and there are many complications, therefore, changes in gut microbial structure and diversity cannot completely explain the mechanism of action of PSPA. Additional functional analyses of the gut microbes and their metabolites should be performed to elucidate their mechanisms of action.

Funding

This work was financially supported by grants from the National Nature Science Foundation of China (No. 81602842), the Natural Science Foundation of Shandong Province (No. ZR2017LH059), and the Health Commission Foundation of Shandong Province (202012020832). Study also supported by Young Backbone Teachers Visiting and Training Program of Binzhou Medical University.

Data availability statement

The sequencing data have been deposited at SRA of the NCBI database under project identification number PRJNA1097665, (the accession numbers of each sample were as follows SAMN40876317, SAMN40876318, SAMN40876319, SAMN40876320, SAMN40876321, SAMN40876322, SAMN40876323, SAMN40876324, SAMN40876325, SAMN40876326, SAMN40876327, SAMN40876328, SAMN40876329, SAMN40876330, SAMN40876331, SAMN40876332, SAMN40876333, SAMN40876334, SAMN40876335, SAMN40876336, SAMN40876337, SAMN40876338, SAMN40876339, SAMN40876340, SAMN40876341, SAMN40876342, SAMN40876343, SAMN40876344, SAMN40876345, SAMN40876346) and other data that support the findings of this study are available in the supplementary material of this article.

Ethics approval and consent to participate

All animal studies were implemented following institutional regulations and approved by the Department of the Experimental Animal Center of Binzhou Medical University (2022- 361).

CRediT authorship contribution statement

Wei Mi: Project administration, Investigation. **Zhiyong Hu:** Visualization, Funding acquisition. **Shuying Zhao:** Visualization, Investigation. **Wei Wang:** Investigation, Data curation. **Wu Lian:** Methodology, Data curation. **Peng Lu:** Writing – review & editing, Investigation. **Tala Shi:** Writing – original draft, Data curation.

Declaration of competing interest

All authors declare that they have no known competing financial interests or personal relationships that could have appeared to

influence the work reported in this paper.

Appendix A. Supplementary data

Supplementary data to this article can be found online at https://doi.org/10.1016/j.heliyon.2024.e31784.

References

[1] K. Ogurtsova, L. Guariguata, N.C. Barengo, P.L.-D. Ruiz, J.W. Sacre, S. Karuranga, H. Sun, E.J. Boyko, D.J. Magliano, IDF Diabetes Atlas: global estimates of undiagnosed diabetes in adults for 2021, Diabetes Res. Clin. Pract. 183 (2022), https://doi.org/10.1016/j.diabres.2021.109118.

[2] P. Saeedi, I. Petersohn, P. Salpea, B. Malanda, S. Karuranga, N. Unwin, S. Colagiuri, L. Guariguata, A.A. Motala, K. Ogurtsova, J.E. Shaw, D. Bright, R. Williams, Diabetes research and clinical Practice, in: Global and Regional Diabetes Prevalence Estimates for 2019 and Projections for 2030 and 2045: Results from the International Diabetes Federation Diabetes Atlas, ninth ed., 2019, https://doi.org/10.1016/j.diabres.2019.107843, 157.

[3] F. De Vadder, P. Kovatcheva-Datchary, D. Goncalves, J. Vinera, C. Zitoun, A. Duchampt, F. Backhed, G. Mithieux, Microbiota-generated metabolites promote metabolic benefits via gut-brain neural circuits, Cell 156 (2014) 84–96, https://doi.org/10.1016/j.cell.2013.12.016.

[4] Y.-Z.C. Fan Zhu, Xinsun Yang, Jinxia Ke, Harold Corke, Anthocyanins, hydroxycinnamic acid derivatives, and antioxidant activity in roots of different Chinese purple-fleshed sweet potato genotypes, J. Agric. Food Chem. 58 (2010) 7588–7596, https://doi.org/10.1021/jf101867t.

[5] J. Zhao, J. Yu, Q. Zhi, T. Yuan, X. Lei, K. Zeng, J. Ming, Anti-aging effects of the fermented anthocyanin extracts of purple sweet potato on Caenorhabditis elegans, Food Funct. 12 (2021) 12647–12658, https://doi.org/10.1039/d1fo02671b.

[6] J. Li, Z. Shi, Y. Mi, Purple sweet potato color attenuates high fat-induced neuroinflammation in mouse brain by inhibiting MAPK and NF-κB activation, Mol. Med. Rep. (2018), https://doi.org/10.3892/mmr.2018.8440.

[7] T. Esatbeyoglu, M. Rodríguez-Werner, A. Schlösser, P. Winterhalter, G. Rimbach, Fractionation, enzyme inhibitory and cellular antioxidant activity of bioactives from purple sweet potato (Ipomoea batatas), Food Chem. 221 (2017) 447–456, https://doi.org/10.1016/j.foodchem.2016.10.077.

[8] J. Jokioja, K.M. Linderborg, M. Kortesniemi, A. Nuora, J. Heinonen, T. Sainio, M. Viitanen, H. Kallio, B. Yang, Anthocyanin-rich extract from purple potatoes decreases postprandial glycemic response and affects inflammation markers in healthy men, Food Chem. 310 (2020), https://doi.org/10.1016/j.foodchem.2019.125797.

[9] Y. Hu, L. Deng, J. Chen, S. Zhou, S. Liu, Y. Fu, C. Yang, Z. Liao, M. Chen, An analytical pipeline to compare and characterize the anthocyanin antioxidant activities of purple sweet potato cultivars, Food Chem. 194 (2016) 46–54, https://doi.org/10.1016/j.foodchem.2015.07.133.

[10] S. Tang, J. Kan, R. Sun, H. Cai, J. Hong, C. Jin, S. Zong, Anthocyanins from purple sweet potato alleviate doxorubicin-induced cardiotoxicity *in vitro* and *in vivo*, J. Food Biochem. 45 (2021), https://doi.org/10.1111/jfbc.13869.

[11] C.-T.Y. Ping-Hsiao Shih, Gow-Chin Yen, Anthocyanins induce the activation of phase II enzymes through the antioxidant response element pathway against oxidative stress-induced apoptosis, J. Agric. Food Chem. 55 (2007) 9427–9435, https://doi.org/10.1021/jf071933i.

[12] E.L. Klein, V., DFT/B3LYP study of the substituent effect on the reaction enthalpies of the individual steps of single electron transfer−proton transfer and sequential proton loss electron transfer mechanisms of phenols antioxidant action 805 (2007) 153–160.

[13] M. Hidalgo, M.J. Oruna-Concha, S. Kolida, G.E. Walton, S. Kallithraka, J.P.E. Spencer, G.R. Gibson, S. de Pascual-Teresa, Metabolism of anthocyanins by human gut Microflora and their influence on gut bacterial growth, J. Agric. Food Chem. 60 (2012) 3882–3890, https://doi.org/10.1021/jf3002153.

[14] M.A. Jackson, S. Verdi, M.-E. Maxan, C.M. Shin, J. Zierer, R.C.E. Bowyer, T. Martin, F.M.K. Williams, C. Menni, J.T. Bell, T.D. Spector, C.J. Steves, Gut microbiota associations with common diseases and prescription medications in a population-based cohort, Nat. Commun. 9 (2018), https://doi.org/10.1038/s41467-018-05184-7.

[15] E. Razmpoosh, A. Javadi, H.S. Ejtahed, P. Mirmiran, M. Javadi, A. Yousefinejad, The effect of probiotic supplementation on glycemic control and lipid profile in patients with type 2 diabetes: a randomized placebo controlled trial, Diabetes Metabol. Syndr.: Clin. Res. Rev. 13 (2019) 175–182, https://doi.org/10.1016/j.dsx.2018.08.008.

[16] J. Qin, Y. Li, Z. Cai, S. Li, J. Zhu, F. Zhang, S. Liang, W. Zhang, Y. Guan, D. Shen, Y. Peng, D. Zhang, Z. Jie, W. Wu, Y. Qin, W. Xue, J. Li, L. Han, D. Lu, P. Wu, Y. Dai, X. Sun, Z. Li, A. Tang, S. Zhong, X. Li, W. Chen, R. Xu, M. Wang, Q. Feng, M. Gong, J. Yu, Y. Zhang, M. Zhang, T. Hansen, G. Sanchez, J. Raes, G. Falony, S. Okuda, M. Almeida, E. LeChatelier, P. Renault, N. Pons, J.-M. Batto, Z. Zhang, H. Chen, R. Yang, W. Zheng, S. Li, H. Yang, J. Wang, S.D. Ehrlich, R. Nielsen, O. Pedersen, K. Kristiansen, J. Wang, A metagenome-wide association study of gut microbiota in type 2 diabetes, Nature 490 (2012) 55–60, https://doi.org/10.1038/nature11450.

[17] P.L.-j. Zhang Man, J.I.A.N.G. Shao-tong, M.O. Yu-wen, Hypolipidemic and antioxidant effects of anthocyanins from purple sweet potato in rats, Food Science 35 (2014) 246–250.

[18] H.S. Montilla Ec, D. Butschbach, S. Baldermann, N. Watanabe, P. Winterhalter, Preparative isolation of anthocyanins from Japanese purple sweet potato (Ipomoea batatas L.) varieties by high-speed countercurrent chromatography, J. Agric. Food Chem. 58 (2010) 9899–9904, https://doi.org/10.1021/jf101898j.

[19] J.G. Zhao, Q.Q. Yan, R.Y. Xue, J. Zhang, Y.Q. Zhang, Isolation and identification of colourless caffeoyl compounds in purple sweet potato by HPLC-DAD-ESI/MS and their antioxidant activities, Food Chem. 161 (2014) 22–26, https://doi.org/10.1016/j.foodchem.2014.03.079.

[20] D. Liu, Y. Ji, K. Wang, Y. Guo, H. Wang, H. Zhang, L. Li, H. Li, S.W. Cui, H. Wang, Purple sweet potato anthocyanin extract regulates redox state related to gut microbiota homeostasis in obese mice, J. Food Sci. 87 (2022) 2133–2146, https://doi.org/10.1111/1750-3841.16130.

[21] A. Hassan, N. Tajuddin, A. Shaikh, Retrospective Case Series of Patients with Diabetes or Prediabetes Who Were Switched from Omega-3-Acid Ethyl Esters to Icosapent Ethyl, Cardiology and Therapy, vol. 4, 2014, pp. 83–93, https://doi.org/10.1007/s40119-014-0032-9.

[22] D. Ra, Pharmacologic therapy for type 2 diabetes mellitus, Ann. Intern. Med. 133 (2000) 73–74.

[23] K. Ogura, M. Ogura, T. Shoji, Y. Sato, Y. Tahara, G. Yamano, H. Sato, K. Sugizaki, N. Fujita, H. Tatsuoka, R. Usui, E. Mukai, S. Fujimoto, N. Inagaki, K. Nagashima, Oral administration of apple procyanidins ameliorates insulin resistance via Suppression of Pro-inflammatory Cytokine expression in liver of diabetic ob/ob mice, J. Agric. Food Chem. 64 (2016) 8857–8865, https://doi.org/10.1021/acs.jafc.6b03424.

[24] S.M. Bowser, W.T. Moore, R.P. McMillan, M.R. Dorenkott, K.M. Goodrich, L. Ye, S.F. O'Keefe, M.W. Hulver, A.P. Neilson, High-molecular-weight cocoa procyanidins possess enhanced insulin-enhancing and insulin mimetic activities in human primary skeletal muscle cells compared to smaller procyanidins, J. Nutr. Biochem. 39 (2017) 48–58, https://doi.org/10.1016/j.jnutbio.2016.10.001.

[25] P. Strugala, O. Dzydzan, I. Brodyak, A.Z. Kucharska, P. Kuropka, M. Liuta, K. Kaleta-Kuratewicz, A. Przewodowska, D. Michalowska, J. Gabrielska, N. Sybirna, Antidiabetic and Antioxidative Potential of the Blue Congo variety of purple potato extract in streptozotocin-induced diabetic rats, Molecules 24 (2019), https://doi.org/10.3390/molecules24173126.

[26] J.J. Holst, S. Madsbad, K.N. Bojsen-Møller, M.S. Svane, N.B. Jørgensen, C. Dirksen, C. Martinussen, Mechanisms in bariatric surgery: gut hormones, diabetes resolution, and weight loss, Surg. Obes. Relat. Dis. 14 (2018) 708–714, https://doi.org/10.1016/j.soard.2018.03.003.

[27] X. Chen, X. Li, X. Zhang, L. You, P.C.-K. Cheung, R. Huang, J. Xiao, Antihyperglycemic and antihyperlipidemic activities of a polysaccharide from Physalis pubescensL. in streptozotocin (STZ)-induced diabetic mice, Food Funct. 10 (2019) 4868–4876, https://doi.org/10.1039/c9fo00687g.

[28] H.J. Kim, K.A. Koo, W.S. Park, D.M. Kang, H.S. Kim, B.Y. Lee, Y.M. Goo, J.H. Kim, M.K. Lee, D.K. Woo, S.S. Kwak, M.J. Ahn, Anti-obesity activity of anthocyanin and carotenoid extracts from color-fleshed sweet potatoes, J. Food Biochem. 44 (2020), https://doi.org/10.1111/jfbc.13438.

[29] F. Les, G. Casedas, C. Gomez, C. Moliner, M.S. Valero, V. Lopez, The role of anthocyanins as antidiabetic agents: from molecular mechanisms to *in vivo* and human studies, J. Physiol. Biochem. 77 (2021) 109–131, https://doi.org/10.1007/s13105-020-00739-z.

[30] S. Cheng-Guang, Z. Shi-Tao, Effect of Procyanidin on expression of SOD and NO in type 2 diabetes mellitus rats with focal Cerebral Ischemia, Chinese Journal of Stroke 2 (2007).

[31] F.H. Karlsson, V. Tremaroli, I. Nookaew, G. Bergström, C.J. Behre, B. Fagerberg, J. Nielsen, F. Bäckhed, Gut metagenome in European women with normal, impaired and diabetic glucose control, Nature 498 (2013) 99–103, https://doi.org/10.1038/nature12198.

[32] K. Forslund, F. Hildebrand, T. Nielsen, G. Falony, E. Le Chatelier, S. Sunagawa, E. Prifti, S. Vieira-Silva, V. Gudmundsdottir, H. Krogh Pedersen, M. Arumugam, K. Kristiansen, A. Yvonne Voigt, H. Vestergaard, R. Hercog, P. Igor Costea, J. Roat Kultima, J. Li, T. Jørgensen, F. Levenez, J. Dore, H. Bjørn Nielsen, S. Brunak, J. Raes, T. Hansen, J. Wang, S. Dusko Ehrlich, P. Bork, O. Pedersen, Disentangling type 2 diabetes and metformin treatment signatures in the human gut microbiota, Nature 528 (2015) 262–266, https://doi.org/10.1038/nature15766.

[33] S.J. Creely, P.G. McTernan, C.M. Kusminski, f.M. Fisher, N.F. Da Silva, M. Khanolkar, M. Evans, A.L. Harte, S. Kumar, Lipopolysaccharide activates an innate immune system response in human adipose tissue in obesity and type 2 diabetes, Am. J. Physiol. Endocrinol. Metabol. 292 (2007) E740–E747, https://doi.org/10.1152/ajpendo.00302.2006.

[34] A. Kashani, A.D. Brejnrod, C. Jin, T. Kern, A.N. Madsen, L.A. Holm, G.K. Gerber, J.-C. Holm, T. Hansen, B. Holst, M. Arumugam, Impaired glucose metabolism and altered gut microbiome despite calorie restriction of ob/ob mice, Animal Microbiome 1 (2019), https://doi.org/10.1186/s42523-019-0007-1.

[35] M. Federici, X. Zhang, D. Shen, Z. Fang, Z. Jie, X. Qiu, C. Zhang, Y. Chen, L. Ji, Human gut microbiota changes reveal the progression of glucose Intolerance, PLoS One 8 (2013), https://doi.org/10.1371/journal.pone.0071108.

[36] G. Dong, N. Xu, M. Wang, Y. Zhao, F. Jiang, H. Bu, J. Liu, B. Yuan, R. Li, Anthocyanin extract from purple sweet potato Exacerbate Mitophagy to ameliorate Pyroptosis in *Klebsiella pneumoniae* infection, Int. J. Mol. Sci. 22 (2021), https://doi.org/10.3390/ijms222111422.

[37] Y. Kyriachenko, T. Falalyeyeva, O. Korotkyi, N. Molochek, N. Kobyliak, Crosstalk between gut microbiota and antidiabetic drug action, World J. Diabetes 10 (2019) 154–168, https://doi.org/10.4239/wjd.v10.i3.154.

[38] L. Brunkwall, M. Orho-Melander, The gut microbiome as a target for prevention and treatment of hyperglycemia in type 2 diabetes: from current human evidence to future possibilities, Diabetologia 60 (2017) 943–951, https://doi.org/10.1007/s00125-017-4278-3.

[39] M.T. Sorbara, E.R. Littmann, E. Fontana, T.U. Moody, C.E. Kohout, M. Gjonbalaj, V. Eaton, R. Seok, I.M. Leiner, E.G. Pamer, Functional and genomic Variation between human-derived Isolates of Lachnospiraceae reveals inter- and intra-species diversity, Cell Host Microbe 28 (2020) 134–146.e134, https://doi.org/10.1016/j.chom.2020.05.005.

[40] E.E.O. Mariana X Byndloss, Fabian Rivera-Chávez, Connor R. Tiffany, Stephanie A. Cevallos, Kristen L. Lokken, Teresa P. Torres, Austin J. Byndloss, Franziska Faber, Yandong Gao, Yael Litvak, Christopher A. Lopez, Gege Xu, Eleonora Napoli, Cecilia Giulivi, Renée M. Tsolis, Alexander Revzin, Carlito B. Lebrilla, Andreas J. Bäumler, Diabetic effect of anthocyanins in streptozotocin-induced diabetic rats through glucose transporter 4 regulation and prevention of insulin resistance and pancreatic apoptosis, Science 357 (2017) 570–575.

[41] L. Zhang, J. Chu, W. Hao, J. Zhang, H. Li, C. Yang, J. Yang, X. Chen, H. Wang, Gut microbiota and type 2 diabetes mellitus: association, mechanism, and translational applications, Mediat. Inflamm. 2021 (2021) 5110276, https://doi.org/10.1155/2021/5110276.

[42] P.D. Cani, W.M. de Vos, Next-generation beneficial microbes: the case of *Akkermansia muciniphila*, Front. Microbiol. 8 (2017) 1765, https://doi.org/10.3389/fmicb.2017.01765.

[43] J. Zhang, Y. Ni, L. Qian, Q. Fang, T. Zheng, M. Zhang, Q. Gao, Y. Zhang, J. Ni, X. Hou, Y. Bao, P. Kovatcheva-Datchary, A. Xu, H. Li, G. Panagiotou, W. Jia, Decreased abundance of *Akkermansia muciniphila* leads to the impairment of insulin secretion and glucose homeostasis in lean type 2 diabetes, Adv. Sci. 8 (2021), https://doi.org/10.1002/advs.202100536.

[44] S. Fujisaka, I. Usui, A. Nawaz, Y. Igarashi, K. Okabe, Y. Furusawa, S. Watanabe, S. Yamamoto, M. Sasahara, Y. Watanabe, Y. Nagai, K. Yagi, T. Nakagawa, K. Tobe, Bofutsushosan improves gut barrier function with a bloom of *Akkermansia muciniphila* and improves glucose metabolism in mice with diet-induced obesity, Sci. Rep. 10 (2020), https://doi.org/10.1038/s41598-020-62506-w.

[45] E.A. Plovier H, C. Druart, C. Depommier, M. Van Hul, L. Geurts, J. Chilloux, N. Ottman, T. Duparc, L. Lichtenstein, A. Myridakis, N.M. Delzenne, J. Klievink, A. Bhattacharjee, K.C. van der Ark, S. Aalvink, L.O. Martinez, M.E. Dumas, D. Maiter, A. Loumaye, M.P. Hermans, J.P. Thissen, C. Belzer, W.M. de Vos, P. D. Cani, A purified membrane protein from *Akkermansia muciniphila* or the pasteurized bacterium improves metabolism in obese and diabetic mice, Nat Med 23 (2017) 107–113, https://doi.org/10.1038/nm.4236.

[46] Y.T. Mitsuo Sakamoto, Yoshimi Benno, Ohkuma Moriya, faecihominis sp Butyricimonas, Butyricimonas paravirosa sp. nov., isolated from human feces, and emended description of the genus Butyricimonas, Int. J. Syst. Evol. Microbiol. 64 (2014) 2992–2997, https://doi.org/10.1099/ijs.0.065318-0, nov.

[47] E.N. Lidia García-Agudo, Butyricimonas virosa: a rare cause of bacteremia, Anaerobe 54 (2018) 121–123121, https://doi.org/10.1016/j.anaerobe.2018.08.001.

[48] H. Sun, P. Zhang, Y. Zhu, Q. Lou, S. He, Antioxidant and prebiotic activity of five peonidin-based anthocyanins extracted from purple sweet potato (Ipomoea batatas (L.) Lam.), Sci. Rep. 8 (2018), https://doi.org/10.1038/s41598-018-23397-0.

[49] J. Mu, J. Xu, L. Wang, C. Chen, P. Chen, Anti-inflammatory effects of purple sweet potato anthocyanin extract in DSS-induced colitis: modulation of commensal bacteria and attenuated bacterial intestinal infection, Food Funct. 12 (2021) 11503–11514, https://doi.org/10.1039/d1fo02454j.

[50] A. Lacombe, S. Tadepalli, C.-A. Hwang, V.C.H. Wu, Phytochemicals in Lowbush Wild blueberry InactivateEscherichia coliO157:H7 by damaging its cell membrane, Foodborne Pathogens and Disease 10 (2013) 944–950, https://doi.org/10.1089/fpd.2013.1504.

[51] M. Wang, Z. Zhang, H. Sun, S. He, S. Liu, T. Zhang, L. Wang, G. Ma, Research progress of anthocyanin prebiotic activity: a review, Phytomedicine 102 (2022), https://doi.org/10.1016/j.phymed.2022.154145.

[52] J. Wang, Y. He, D. Yu, L. Jin, X. Gong, B. Zhang, Perilla oil regulates intestinal microbiota and alleviates insulin resistance through the PI3K/AKT signaling pathway in type-2 diabetic KKAy mice, Food Chem. Toxicol. 135 (2020) 110965, https://doi.org/10.1016/j.fct.2019.110965.

[53] T. Xia, C.S. Liu, Y.N. Hu, Z.Y. Luo, F.L. Chen, L.X. Yuan, X.M. Tan, Coix seed polysaccharides alleviate type 2 diabetes mellitus via gut microbiota-derived short-chain fatty acids activation of IGF1/PI3K/AKT signaling, Food Res. Int. 150 (2021) 110717, https://doi.org/10.1016/j.foodres.2021.110717.

[54] J. Tan, C. McKenzie, M. Potamitis, A.N. Thorburn, C.R. Mackay, L. Macia, The role of short-chain fatty acids in health and disease, Adv. Immunol. 121 (2014) 91–119, https://doi.org/10.1016/B978-0-12-800100-4.00003-9.

[55] N.S.A. Rosli, S. Abd Gani, M.E. Khayat, U.H. Zaidan, A. Ismail, M.B.H. Abdul Rahim, Short-chain fatty acids: possible regulators of insulin secretion, Mol. Cell. Biochem. 478 (2023) 517–530, https://doi.org/10.1007/s11010-022-04528-8.

[56] H. Yadav, J.H. Lee, J. Lloyd, P. Walter, S.G. Rane, Beneficial metabolic effects of a probiotic via butyrate-induced GLP-1 hormone secretion, J. Biol. Chem. 288 (2013) 25088–25097, https://doi.org/10.1074/jbc.M113.452516.

[57] A. Psichas, M.L. Sleeth, K.G. Murphy, L. Brooks, G.A. Bewick, A.C. Hanyaloglu, M.A. Ghatei, S.R. Bloom, G. Frost, The short-chain fatty acid propionate stimulates GLP-1 and PYY secretion via free fatty acid receptor 2 in rodents, Int. J. Obes. 39 (2015) 424–429, https://doi.org/10.1038/ijo.2014.153.

[58] D.A. Luna-Vital, L. Chatham, J. Juvik, V. Singh, P. Somavat, E.G. de Mejia, Activating effects of Phenolics from Apache red Zea mays L. On free fatty acid receptor 1 and glucokinase evaluated with a dual culture system with epithelial, pancreatic, and liver cells, J. Agric. Food Chem. 67 (2019) 9148–9159, https://doi.org/10.1021/acs.jafc.8b06642.

[59] A.L. Cunningham, J.W. Stephens, D.A. Harris, Gut microbiota influence in type 2 diabetes mellitus (T2DM), Gut Pathog. 13 (2021) 50, https://doi.org/10.1186/s13099-021-00446-0.